Optical heterodyne measurement of pulsed lasers: Toward high-precision pulsed spectroscopy

Michale S. Fee, K. Danzmann,* and Steven Chu
Department of Physics, Stanford University, Stanford, California 94305
(Received 12 March 1990; revised manuscript received 23 October 1991)

In this paper we explore theoretically and experimentally the effect of fluctuations in the instantaneous frequency of a pulsed laser on the shape and position of two-photon transition spectra. The usual procedure of characterizing a pulsed laser by its frequency energy spectrum is insufficient for precision measurements. The nonlinear nature of the two-photon transition produces a systematic shift of the atomic spectrum with respect to the laser frequency spectrum that is dependent on the phase evolution of the laser pulse. In fact, any nonlinear process (e.g., second-harmonic generation) may result in displaced or distorted spectra. We also find that Fabry-Pérot filtering a laser pulse can result in large frequency chirps. We use an optical heterodyne technique to measure the instantaneous frequency of our excimer-pumped dye-laser system to an uncertainty of 1.3 MHz and determine the effect of the inherent frequency chirps of this system on a two-photon transition. We conclude that with this technique, precision nonlinear spectroscopy to the level of 1 MHz may be achieved with pulsed lasers.

PACS number(s): 42.60.Gd

I. INTRODUCTION

In an increasing number of applications with pulsed lasers, the interpretation of an experiment can be limited by the fact that these laser sources are generally not Fourier-transform limited and can have complex spectral character. Examples of such applications include precision spectroscopy, coherent transient spectroscopy, and stimulated Raman spectroscopy. In the most demanding applications, researchers work hard to avoid pulsed lasers. The highest-resolution laser spectroscopy is done with cw lasers, and in experiments where the "pulse" aspect of the laser sources is essential, a cw laser was suddenly gated on with an acousto-optic or electro-optic modulator, or the frequency of the relevant transition was quickly switched, etc. Unfortunately, there are many applications where pulsed lasers are unavoidable. In much of the ultraviolet, vacuum ultraviolet, and infrared range of the spectrum, good cw laser sources do not exist. Also, in applications where the oscillator strengths are too weak to be sufficiently excited with cw sources, the imperfect pulsed laser is all that we have.

Pulsed lasers are usually characterized in terms of their temporal and spectral intensity profiles. Any frequency fluctuations appear as a spectral broadening of the laser output, which is expressed by the degree to which the laser is not Fourier-transform limited. Apart from picosecond and femtosecond lasers where the pulses can actually be very close to the Fourier-transform limit, most lasers fall short of achieving the minimum uncertainty in $\Delta\nu\Delta t$. As a concrete example, suppose a narrowband pulsed laser is constructed by amplifying a cw laser with a series of traveling-wave amplifiers. The process of amplifying a pulsed laser inherently involves rapid changes in the gain. Thus the index of refraction of the amplifying medium is rapidly modulated, resulting in fluctuations of the laser frequency within a single pulse. Measurement of the spectral broadening that results from the induced frequency modulation does not tell us the instantaneous frequency (the time derivative of the instantaneous phase of the complex amplitude) of the pulse. This additional information is essential to thoroughly predict or interpret the results of several types of experiments. This fact was recognized and discussed by Wieman and Hänsch [1], and was the principle uncertainty in their measurement of the hydrogen $1S$ Lamb shift.

Any spectroscopic measurement involving processes that are higher order in the laser-field interaction will be sensitive to the time development of the laser frequency. These include measurements made at saturating intensities, multiphoton transitions, harmonic generation, and parametric down conversion. In addition, this information is needed in spectroscopic experiments where some temporal piece of the laser pulse is more effective in producing signal, or when there is some degree of time resolution within one pulse, such as when atomic states are rapidly decaying. This will emphasize one portion of the laser pulse over another, making the knowledge of the instantaneous frequency versus time essential.

In this paper, we will explore theoretically the effect of fluctuations in the instantaneous frequency $F(t)$ of a pulsed laser on the shape and position of two-photon transitions. Because of the simplicity of eliminating first-order Doppler shifts, this transition is of particular interest in the field of precision spectroscopy, as evidenced by recent pulsed measurements of the $1S$-$2S$ two-photon transition in hydrogen, positronium, and muonium [1–6]. We will show that the detailed spectral behavior of the laser source must be known before a reliable high-resolution measurement can be made.

We experimentally measure the instantaneous frequency behavior of our excimer-pumped dye-laser system and determine the effect of the inherent frequency chirps of this system on a two-photon transition. In addition, we have experimentally investigated the effect of filtering this pulsed laser with a Fabry-Pérot filter, since this technique

to reduce the laser bandwidth has been widely used in precision pulsed measurements [3,4,6]. In the case of hydrogen, there is a discrepancy between the pulsed measurement and the subsequent continuous-wave measurements [7,8]. We propose an approximate correction to the pulsed hydrogen measurement that brings that result into good agreement with the theoretical result.

II. TWO-PHOTON SPECTRA WITH NON-FOURIER-TRANSFORM-LIMITED PULSES

In the pulsed spectroscopy of transitions that are first order in the atom-field interaction (i.e., one-photon transitions), the experimental line shape is easily predicted; it is just the convolution of the atomic line shape and the spectral intensity (or power spectrum) of the incident radiation. The power spectrum $I(\omega)$ is proportional to $|\int E(t)e^{-i\omega t}dt|^2$, where $E(t)$ is the complex instantaneous electric field of the laser [9]. This is typically measured using a high-resolution interferometer (an optical spectrum analyzer), which may be calibrated with an optical frequency reference such as a molecular-vapor line. Since the line shape is readily predicted, there is no ambiguity in measuring the atomic transition frequency.

When the observed transition is second order (or higher) in the atom-field interaction (i.e., a two-photon transition), the spectral intensity of the incident laser is no longer sufficient information to predict the shape of the observed spectrum. The result is ambiguity in determining the atomic transition frequency.

To ascertain the effect of frequency chirps on the two-photon line shape, we have numerically solved the equations of motion for the interaction picture atomic amplitude coefficients. These were obtained from the results of the conventional second-order, semiclassical calculation of this transition. In the electric dipole approximation, the Hamiltonian is

$$\hat{H}_{ij}=\mathbf{d}_{ij}\cdot\mathbf{E}(\mathbf{r},t)$$

where $\mathbf{E}(\mathbf{r},t)=\hat{\xi}E(\mathbf{r},t)e^{-i\omega t}$, $\hat{\xi}$ is the polarization unit vector of the incident field, and $\mathbf{d}_{ij}$ is the electric dipole matrix element. The Schrödinger picture probability amplitudes, $c_a(t)$ for the excited state and $c_b(t)$ for the ground state, are given by [10]

$$\dot{c}_a(t)=-i[\omega_a+\Delta\omega_a(t)]c_a(t)-\frac{i}{h}V_{ab}(t)c_b(t) \tag{1a}$$

and

$$\dot{c}_b(t)=-i[\omega_b+\Delta\omega_b(t)]c_b(t)-\frac{i}{h}V_{ba}(t)c_a(t)\ , \tag{1b}$$

where

$$\Delta\omega_a(t)=-i\frac{\Gamma_a}{2}+\left[\frac{ea_0}{2\hbar}\right]^2\sum_n\left[\frac{|\mathbf{d}_{an}\cdot\mathbf{E}^*(\mathbf{r},t)|^2}{\omega_{an}+\omega}+\frac{|\mathbf{d}_{an}\cdot\mathbf{E}(\mathbf{r},t)|^2}{\omega_{an}+\omega}\right], \tag{2}$$

and

$$\frac{V_{ab}(t)}{\hbar}=e^{-i2\omega t}\left[\frac{ea_0}{2\hbar}\right]^2\sum_n\frac{d_{an}\cdot\mathbf{E}(\mathbf{r},t)\mathbf{d}_{nb}\cdot\mathbf{E}(\mathbf{r},t)}{\omega_{bn}+\omega} \tag{3}$$

is the second-order interaction potential, $\hbar\omega_a$ is the energy eigenvalue of the excited state $|a\rangle$, and Γ_a is the decay rate to other levels. $\Delta\omega_b(t)$ is defined similarly to $\Delta\omega_a(t)$.

These equations can be represented in the interaction picture with quantities containing no optical frequencies:

$$\dot{C}_a(t)=-i\Delta\omega_a(t)C_a(t)-\frac{i}{\hbar}V'_{ab}(t)e^{-i\Omega t}C_b(t)\ , \tag{4a}$$

$$\dot{C}_b(t)=-i\Delta\omega_b(t)C_b(t)-\frac{i}{\hbar}V'_{ba}(t)e^{i\Omega t}C_a(t)\ , \tag{4b}$$

where the detuning $\Omega=2\omega-\omega_{ab}$, $\omega_{ab}=\omega_a-\omega_b$, $C_a(t)=e^{i\omega_a t}c_a(t)$, and $V'_{ab}(t)=e^{i2\omega t}V_{ab}(t)$. These equations can be solved using a simple forward stepping integration routine to determine the line shape of the two-photon transition.

A. Simplifying assumptions

Under certain conditions, which we will relax later, these equations simplify considerably. If we assume that there is no decay from the excited or ground states and we assume that the intensity is sufficiently low that there is a negligible Stark shift, the first term in the right-hand sides of Eqs. (4a) and (4b) can be neglected. If we assume additionally that the excitation time is sufficiently small that there is negligible depopulation of the ground state, then (4b) can also be neglected and we can set $C_b(t)=1$. Thus

$$\dot{C}_a(t)=-\frac{i}{\hbar}V'_{ab}(t)e^{-i\Omega t} \tag{5}$$

and integrating, we find the final-state population after the excitation [11]:

$$\rho_a(\Omega)=\left|-\frac{i}{\hbar}\left[\frac{ea_0}{2\hbar}\right]^2\sum_n\frac{\mathbf{d}_{an}\cdot\hat{\xi}\mathbf{d}_{nb}\cdot\hat{\xi}}{\omega_{bn}+\omega}\right|^2\times\left|\int_{-\infty}^{\infty}E^2(t)e^{-i\Omega t}dt\right|^2. \tag{6}$$

The assumption here is that the excitation is of finite extent in time, and we measure the final-state population after the excitation is over.

Under these conditions, $\rho_a(\Omega)$ is proportional to the Fourier power spectrum of the squared electric field $E^2(t)$. However, without complete knowledge of $E(t)$, we may have simplistically predicted the line shape to be the power spectrum of the incident radiation $I(\omega)=|\int E(t)e^{-i\omega t}dt|^2$. For example, if the center of gravity (CG) of the incident radiation is found to be at a frequency ω_0, the CG of the two-photon line shape might be assumed to be found at $2\omega_0$. In general, however, $E(t)$ and $E^2(t)$ do not have the same power spectrum, and the CG (and peak) of the two-photon line shape may be shifted with respect to the CG of the power spectrum of the

incident radiation. The result would be an incorrect identification of the atomic resonance frequency.

To demonstrate the magnitude of this effect, Fig. 1 shows the shift ($\Delta\nu$) of the two-photon line center relative to the full two-photon transition frequency resulting from excitation with a non-Fourier-transform-limited pulse. The shift is calculated as $\Delta\nu=\nu''-2\nu'$ where ν' is the center of the power spectrum of $E^2(t)$ and ν' is the center of the power spectrum of $E(t)$. In this way, the arbitrary choice of the center frequency of the envelope $E(t)$ does not enter into the results.

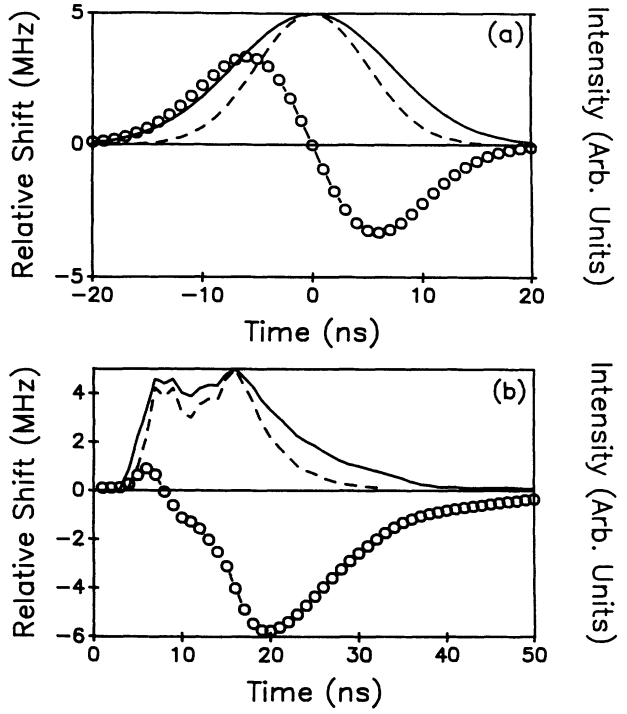

FIG. 1. Shift of the two-photon line center relative to the two-photon transition frequency (open circles) resulting from excitation with a non-Fourier-transform-limited pulse. As described in Sec. II, we model the two-photon line shape as the power spectrum of the square of the incident complex electric field envelope $E(t)$. The relative shift is found by comparing the center of gravity of this line shape to the center of the incident power spectrum. (a) The incident field has the Gaussian intensity profile shown (solid curve). The frequency of the field starts at $+10$ MHz detuning and then jumps abruptly to -10 MHz at some time τ during the pulse. The shift is plotted as a function of the time τ at which the frequency jump occurs under the pulse. Intuitively, the shift can be understood as follows. The two-photon transition rate is proportional to $I^2(t)$ (dashed curve). Thus the line shape reflects the instantaneous frequency of the pulse at time t weighted by $I^2(t)$. The power spectrum of the incident field weights the instantaneous frequency by $I(t)$. For example, if the frequency jump occurs at time $\tau=6$ ns, the two-photon line shape will more heavily reflect the $+10$-MHz frequency at the peak intensity than will the power spectrum of the pulse. The result is that the center of gravity of the two-photon line shape appears roughly 3 MHz below the two-photon transition frequency. (b) The incident pulse has the experimentally measured intensity profile (solid line) of an excimer-pumped dye-amplifier pulse. We show the shift assuming the frequency jumps at time τ, as described for (a). This demonstrates that sudden steps in the intensity profile (i.e., the rising edge of the pulse) do not produce shifts in the two-photon spectra. A long trailing edge, however, can result in large shifts.

In Fig. 1(a), the incident field has a Gaussian intensity profile. The frequency of the field envelope starts at $+10$ MHz and then jumps abruptly to -10 MHz at a time τ during the pulse. Although this step-function frequency chirp seems artificial, it clearly demonstrates the source of the shift. In addition, if one filters a pulse in a Fabry-Pérot filter incorrectly, one obtains a chirp quite similar to this step function.

The shift in Fig. 1 is plotted as a function of the time τ at which the frequency jumps under the pulse. When τ is much larger than the pulse width τ_0, the frequency is constant throughout the pulse; thus the spectrum of $E(t)$ is centered at $\nu'=+10$ MHz, the spectrum of $E^2(t)$ is centered at $\nu''=+20$ MHz, and the relative shift is therefore $\Delta\nu=\nu''-2\nu'=0$. When the frequency jumps at the center of the pulse ($\tau=0$), then $\nu'=\nu''=0$ and there is no relative shift in the spectra of these two signals.

In the region where τ is positive and on the order of τ_0, the center of the power spectrum of both $E(t)$ and $E^2(t)$ will be shifted to some positive frequency, as expected. Note, however, that the squared field intensity profile $I^2(t)=|E^2(t)|^2$ is $\sqrt{2}$ narrower than the field intensity $I(t)=|E(t)|^2$ for our Gaussian pulse; consequently the pulse energy of $E^2(t)$ is concentrated at times less than τ where the frequency of the squared field is $+20$ MHz. Conversely, the field $E(t)$ has a larger fraction of its energy times greater than τ, where the frequency is -10 MHz. Thus the power spectrum of $E^2(t)$ appears at a frequency higher by $\Delta\nu$.

Using the preceding arguments, it can be shown that if the instantaneous frequency $F(t)=\dot{\phi}(t)$ is symmetric or antisymmetric with respect to the peak of the Gaussian pulse, there will be no shift of the two-photon line shape relative to the spectrum of the exciting field. For example, a linearly chirped Gaussian pulse will not produce a shift in a two-photon line shape.

If the step-function chirp is imposed on a measured, pulse-amplified dye-laser intensity profile instead of a Gaussian intensity profile, the relative shift in the CG of the power spectrum of $E(t)$ and $E^2(t)$ is strongly asymmetric, as shown in Fig. 1(b). The large shifts associated with frequency chirps under the long, low-intensity tail of a pulse result because the relative energy under the long tail is greatly decreased when the field is squared. The relative energy under the sharp feature remains roughly unchanged, resulting in only small shifts in the spectrum. A limiting case is a square pulse, which will not produce any shifts of the sort we have been discussing since its shape does not change when the field is squared.

B. Real atomic systems

The constraints used to obtain (6) are fairly restrictive in real atomic systems and experimental situations. If these restrictions are not satisfied then Eqs. (4) must be used to obtain the two-photon line shape. There may be

a contribution to the shift from each of the terms that were eliminated from Eq. (4). We will discuss each of these contributions. We will not, however, discuss interactions between these various terms, which may not be additive in the shift they produce.

If the presence of ground-state decay (as in positronium) results in a natural linewidth of Γ_b, then the two-photon line shape is given by

$$\rho(\Omega) \propto \left| \int_{-\infty}^{\infty} E_i^2(t) e^{-(\Gamma_b/2)t} e^{-i\Omega t} dt \right|^2 . \quad (7)$$

Equation (7) is obtained by substituting an exponentially decaying factor for the ground-state amplitude $C_b(t)$ in (4a). The effect of the decaying exponential inside the integral is clear. Since the rate of population transfer to the excited state is proportional to the ground-state population, a decreasing ground-state population will make the trailing edge of the pulse less important to the resulting line shape. In the limit that the ground-state lifetime is much shorter than the excitation pulse, only the frequency of the excitation pulse at the time when the ground state is present will determine the center frequency of the measured atomic line. The decaying exponential is just a weighting factor that reflects this fact. The center of the measured line will therefore be different than if there were no atomic decay.

In the presence of excited-state decay, the situation is somewhat different. Using Eq. (4a), and making the substitution $C_a'(t) = C_a(t) e^{(\Gamma_a/2)t}$, we find that at some measurement time τ_m after the excitation, the excited-state population is

$$\rho_a(\Omega, \tau_m) \propto e^{-\Gamma_a \tau_m} \left| \int_{-\infty}^{\tau_m} E^2(t) e^{+(\Gamma_2/2)t} e^{-i\Omega t} dt \right|^2 . \quad (8)$$

In the case where the final-state population is measured at some time τ_m after the excitation pulse (e.g., if atoms in the excited state are photoionized by a second laser pulse), the situation is similar to that described above. In this case, however, the excited state is decaying, so that before the excited state is photoionized, a larger fraction of transitions that occurred early in the excitation pulse will have decayed than those that occurred later in the pulse. Thus the frequencies of the trailing edge of the excitation pulse will be more significant in determining the line shape, and the measured line center will again be different than if there were no atomic decay present. If detection of excited-state population is achieved by field quenching or collisional transfer, where the transition rate is measured rather than the total transferred population, there is no relative shift in the line center caused by excited-state decay.

Another important case occurs when the photoionization of the excited state is due to the pulse that is driving the two-photon transition. If the photoionization rate is much higher than the excited-state decay rate, there will be no effect on the line shape due to excited-state decay, just as for detection for field quenching. However, if the photoionizing rate is comparable to the decay rate, there will be a shift induced by decay of the excited state. Even if there is no excited-state decay, there is another source of shift. Because the photoionization rate is intensity dependent, detected atoms will most likely have been ionized during the most intense part of the driving (and photoionizing) pulse. This deemphasizes the transitions that occur in the trailing edge of the pulse, making the frequency of the pulse at the trailing edge less important. This effect has a complicated dependence on the driving pulse and the photoionization cross section and so must be modeled for the experiment under consideration.

A final situation we will discuss is the case where there is no decay of the excited or ground states, and the transition is driven with an intense laser pulse, such that the final-state population approaches one. To study this behavior we use a model laser pulse whose steep rising edge goes as $e^{-\gamma(t-t_0)^4}$ and whose slower falling edge goes as $e^{-\gamma(t-t_0)^2}$. The pulse is given a linear chirp making the pulse width roughly two times the Fourier-transform limit. The final excited-state population is then found by numerically integrating the full equations of motion for the two-photon transition driven by this pulse. The first terms on the right-hand sides of Eqs. (4a) and (4b), those contributing to the ac Stark effect, are set to zero to separate this shift in the line from that due to saturation.

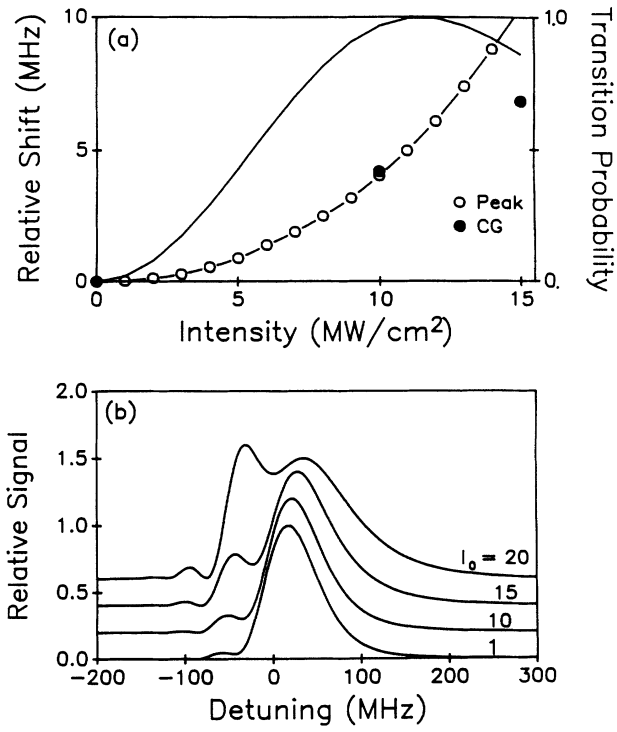

FIG. 2. Effects of high-intensity driving fields on the two-photon line center and line shape. The driving pulse is an asymmetric Gaussian-like pulse with a linear frequency chirp (see text). The terms contributing to ac Stark effect are turned off to show only the effect of the frequency chirp in the coherent interaction between the ground and excited states. (a) The additional shift in the peak (open circles) and center of gravity (filled circles) of the two-photon line is shown as a function of peak intensity of the driving field. Also shown (solid line) is the final excited-state population after the pulse. (b) The two-photon line shape is shown at four peak intensities of the driving field: $I_0 = 1.0$, 10, 15, and 20 MW/cm^2.

The line shape and center of gravity of the line are found for a range of intensities resulting in final excited-state populations near one.

Figure 2(a) shows the shift imposed on the line center as a function of peak intensity. Since the pulse we are using is asymmetric and has a frequency chirp, we expect a shift at low intensity due to the presence of $E^2(t)$ in the interaction Hamiltonian. This shift ($\sim$20 MHz) is subtracted off to make clear the additional shift due solely to the coherent interaction between the ground and excited states at high intensity. The total transition probability is also shown in Fig. 2(a).

As the transition probability approaches one, this additional shift tends to increase with intensity until after the peak transition probability has reached one. At even higher intensities the behavior becomes more complicated, and since for precision measurements it is rarely important to use such intense fields, we do not include these points. We can give an estimate of these high-intensity effects on the two-photon line center, but have been unable to explain them intuitively. The effect of high intensity on the line shape of positronium is shown in Fig. 2(b). In an actual experiment, however, the line shape is most likely an average over those shown, suitably weighted for a Gaussian transverse intensity profile.

III. MEASUREMENT OF PULSED LASER ELECTRIC FIELD

For the purposes of discussion, we have previously assumed several analytical forms for the frequency behavior of a pulse (i.e., a step function or a linear chirp). In an actual precision measurement, however, this is not a sufficient approximation to a real laser pulse; one must measure the frequency behavior of the laser used. In general, pulsed lasers have spatial variation of both the magnitude and phase of the wave front that deviates from an ideal Gaussian.

For example, frequency differences of 10–20 MHz at opposite transverse locations on the beam have been observed with our laser, corresponding to an angular rotation of the propagation direction at the laser output. In principle, to fully characterize a pulsed laser source, one must map the complex electric field at various transverse locations of the beam.

One can see that spatial variations of the instantaneous laser frequency need to be determined for nonlinear spectroscopy for the same reason that temporal variations must be determined; the spatially averaged optical spectrum is not the same as the spatially averaged nonlinear atomic response. However, a precision measurement will generally involve filtering the pulsed laser with a Fabry-Pérot resonator, greatly reducing the problem of spatial incoherence of the pulsed laser.

This can be demonstrated as follows: A linear spatial variation of the laser frequency is the dominant contribution in our system due to the transverse dye pumping geometry. Since this variation is odd with respect to inversion through the optic axis of a mode-matched filter cavity, this disturbance will not be transmitted by a confocal Fabry-Pérot cavity tuned to resonance on the even-order modes. If even-order contributions to the phase front variations are large enough to be a problem, then a nonconfocal cavity can be used as long as higher-order modes are sufficiently spaced from the TEM_{00} mode not to pass power from the wings of the pulsed laser spectrum. If spatial frequency variations are a problem in an application with no Fabry-Pérot filter, the measurement techniques presented in this paper are applicable to making an appropriate characterization of the laser field.

The instantaneous electric field of a pulsed laser can be measured, including its phase relative to a reference laser, by heterodyning the pulsed laser and the reference laser. The two laser fields are combined at a beam splitter, and a detector placed in some small region of the resulting wave. If we consider all quantities to be those found at the center of the detector, then the cycle-averaged intensity

$$I \propto |E_p(t)+E_{\mathrm{ASE}}(t)+E_{\mathrm{cw}}e^{i\omega m t}|^2 \tag{9}$$

where the incident pulsed laser electric field is given by $\tilde{E}_p(t)=\hat{\xi}\,\mathrm{Re}[E_p(t)e^{-i\omega_0 t}]$, the electric field noise in the pulsed laser due to amplified spontaneous emission (ASE) is $\tilde{E}_{\mathrm{ASE}}(t)=\hat{\xi}\,\mathrm{Re}[E_{\mathrm{ASE}}(t)e^{-i\omega_0 t}]$, and the electric field of the reference laser is $\tilde{E}_{\mathrm{cw}}(t)=\hat{\xi}\,\mathrm{Re}[E_{\mathrm{cw}}(t)e^{-i(\omega_0-\omega_m)t}]$. The angular frequency ω_0 is some appropriately chosen center frequency, and ω_m is the offset between the cw reference wave and ω_0.

A. Experimental apparatus

In the current experimental setup (Fig. 3), a Coherent 699-21 actively stabilized, continuous-wave (cw), ring dye laser serves as a frequency stable ($\sim$1 MHz rms) source of 486-nm radiation. This wavelength is used since the original intent of this experiment was to excite the $1S$-$2S$ two-photon transition in Ps. The cw laser is used for three primary purposes: a reference beam for the heterodyning, an injection seed beam for up to four stages of a modified Lambda-Physik pulsed dye amplifier, and an optical reference to frequency lock a Fabry-Pérot filter cavity to the center of the pulsed amplifier output. A FM locking scheme is used to stabilize the filter cavity to 0.5 MHz [12,13]. The amplifier is pumped with 20-ns, $\sim$400-mJ pulses from a Lambda-Physik excimer laser.

We have overcome several severe difficulties encountered with the simple arrangement of beam splitting the cw laser for each of these functions. When the pulsed amplifier fires, there is a light pulse ($\sim$50 μJ) that back propagates along the seed beam. If this radiation is allowed to enter the cw ring laser, it causes the laser to reverse the lasing direction for some period of time ($\sim$0.1 s) sufficient for the servo loops of the active stabilization to lose lock, or for the laser to mode hop. We remove most of this back-propagating pulse by focusing the seed beam through a pinhole sufficiently large that 90% of the laser power is passed; the seed beam is then recollimated, sent through a Brewster prism, and sent into the pulsed amplifier. The pulse returning along the seed beam is thus dispersed in the prism, and the large portion of this pulse that is amplified spontaneous emission, with its

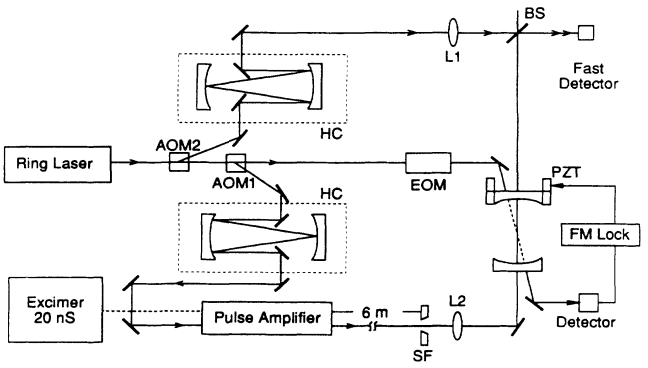

FIG. 3. Experimental setup. Acousto-optic modulator AOM2 switches the cw laser into a 2.3-m Herriot cell (HC) optical delay line (85 ns) to serve as the cw optical frequency reference for heterodyning. AOM1 switches the laser into another optical delay line to serve as the seed beam for the excimer-pumped dye amplifier. The pulsed beam is spatially filtered (SF) and mode matched into a Fabry-Pérot filter cavity. The filtered pulses are sent onto the fast photodiode with the reference beam and the interference signal is digitized. The filter cavity is stabilized to an off-axis cw beam using a FM locking technique. An electro-optic modulator (EOM) generates the 6-MHz optical sidebands used in the cavity locking scheme.

large wavelength spread, cannot pass through the pinhole.

Due to light scattered from the seed beam by optics and dust in the amplifier that is subsequently amplified backwards through the amplifier, there is a large component of light in this pulse at the seed frequency that passes back through the pinhole ($\sim < 10$ μJ). Thus even with this technique a sufficient amount of pulsed light reaches the ring laser to produce a significant disturbance, as evidenced by occasional dropouts in the ring laser output of up to 1 μs duration after the pulsed laser fires. More often the ring laser output exhibits large oscillations at the longitudinal mode spacing (180 MHz) for roughly the same duration. This is presumably due to transient excitation of adjacent longitudinal modes when the back-propagating pulse from the amplifier enters the ring laser.

To eliminate this problem, the seed beam is extracted from the ring laser output with a 40-MHz tunable acousto-optic modulator (AOM1). Since the seed beam only needs to be on for the duration of the excimer pump pulse, switching AOM1 on and then rapidly off allows us to divert 80% of the cw laser beam into the seed beam, then close the optical path in time that the back-propagating pulse cannot enter the ring laser. A 2.3-m, 12-pass Herriott cell [14] delay line (85 ns) is placed in the light path between AOM1 and the pulsed amplifier to allow for the 50-ns (90% to 10%) turnoff time of our AOM. This is sufficient to eliminate dropouts in the ring laser, although because of the nonideal turnoff characteristics of the AOM, it does not entirely eliminate transient oscillations. A Herriott cell is used since it allows for long optical delays with negligible diffraction loss.

Because of stray pulsed light, and to some extent the residual transient oscillations, it is necessary to extract the heterodyning beam from the cw source prior to the firing of the pulsed amplifier. This is accomplished with another acousto-optic modulator (AOM2), driven by a crystal controlled 110-MHz rf source, placed before AOM1. AOM2 is double passed to produce a -220-MHz shift with respect to the carrier. This is sent into a 140-ns delay line (2.3-m, 20-pass Herriott cell), and then through additional AO modulators to produce the desired beat frequency with the pulsed laser. Since we use one Herriott cell for both of the delay lines discussed, the heterodyning beam must be focused through a pinhole to remove a small amount of scattered light in the Herriott cell due to the back-propagating ASE in the seed beam. AOM2 is turned on one microsecond before the pulsed amplifier fires to fill up the heterodyning beam delay line. It is turned off 100 ns before the amplifier fires, to allow the light to pass through AOM1 into the seed beam.

The 70-mJ amplified pulses are propagated $\sim$6 m to the spatial Fourier plane [15] of the final amplifier stage output and passed through an aperature to remove high spatial frequency components of the beam. The filter, which passes roughly 80% of the beam energy, primarily serves to protect a filter cavity from beam hot spots.

The pulsed beam is then attenuated and sent collinearly with the reference beam onto a 2-GHz bandwidth silicon photodiode detector. The photodiode is ac coupled to a pulse optimized rf amplifier to yield 30-dB gain between 100 kHz and 750 MHz. The output of the detector

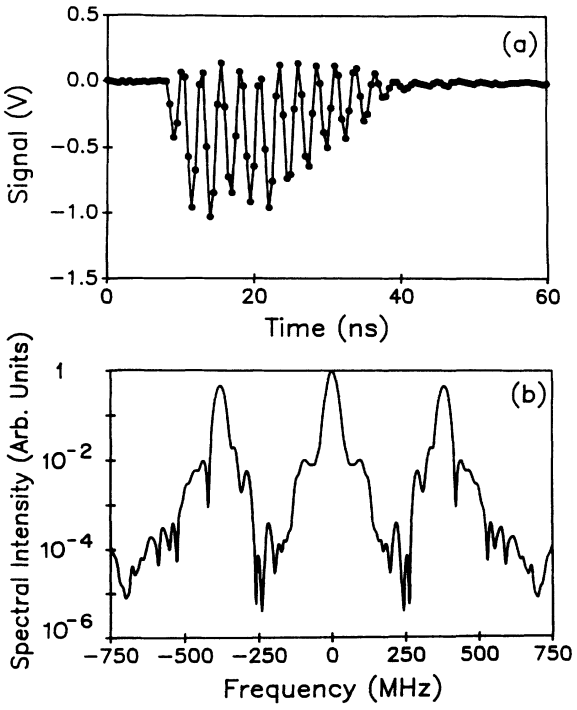

FIG. 4. (a) Typical heterodyne signal of an excimer-pumped dyne-amplifier pulse. Solid circles show digitized points. (b) A double-sided fast-Fourier transform of heterodyne signal shows the peak at dc associated with the pulse intensity term, and peaks at $\pm$380 MHz associated with the interference terms.

amplifier is digitized by a Tektronix DSA 602 digital oscilloscope (2 Gsample/s sampling rate, 5.9 effective bits at 400 MHz) and the resulting digitized signal is transferred to a computer for processing. A typical digitized heterodyne signal at 380 MHz is shown in Fig. 4(a).

The intensity of the cw reference beam is constant over the time scale of 20–100 ns, thus this term does not appear in our amplified signal. Amplified spontaneous emission accounts for roughly 10% of the integrated pulse energy for typical alignment of the pulsed amplifier. However, since it is spectrally broad (10 nm), its spectral intensity is at the 10^{-5} to 10^{-6} level below the amplified signal, and its contribution to interference terms is negligible compared to other noise sources. We will refine our definition of $E_p(t)$ given in (4): $E_p(t)$ is that component of the pulsed electric field that contributes to the interference signal of the pulsed and cw light within the bandwidth of our detection scheme, and $E_{\mathrm{ASE}}(t)$ is the component that contributes only a low-frequency intensity term $I_{\mathrm{ASE}}(t)$.

B. Electric field reconstruction algorithm

From (9), the expression for the digitized signal is

$$V=I_p(t)+I_{\mathrm{ASE}}(t)+2|E_p(t)|\,|E_{\mathrm{cw}}|\cos\phi(t) \tag{10}$$

where $\phi(t)$ is the phase of the pulsed light relative to the reference field. This signal contains three unknown quantities associated with the pulse. It is not possible in general to extract the required phase and intensity information from this signal. However, with a sufficiently high beat note, certain assumptions can be made about the three time-dependent terms in (10), and all of the information required to extract the instantaneous phase of a pulse can be obtained with a single detector.

If we rewrite (10) in the following (time domain) form:

$$V=I_p'(t)+E_p(t)E_{\mathrm{cw}}^{*}e^{-i\omega_m t}+E_p^{*}(t)E_{\mathrm{cw}}e^{i\omega_m t} \tag{11}$$

where $I_p'(t)=I_p(t)+I_{\mathrm{ASE}}(t)$, it becomes clear how to extract the electric field of the pulse. Under the assumption that the beat note is at a sufficiently high frequency that the frequency components of the interference terms are well separated in the Fourier domain from those associated with the intensity profile, the Fourier transform of this signal consists of the three distinct terms, as shown in Fig. 4(b) for the case of a measured beat note for our dye-laser system. The term centered at the origin is associated with the pulse intensity. The positive frequency component of the interference term, corresponding to the second term in (11), is centered at $+\omega_m$, and the negative frequency component of the interference term, corresponding to the third term in (11), is centered at $-\omega_m$. If the beat frequency ω_m is sufficiently large that there is little overlap between these terms in the frequency domain, the second term in (11) may be extracted with a bandpass filter of half-width $\omega_m/2$, centered at $+\omega_m$.

The filter can be one of several types. A rectangular filter maximizes the information content of the filtered signal, but introduces characteristic sidelobes in the time domain, making interpretation of the time domain results difficult. A Blackman filter, given by

$$\Gamma(\omega)=\left[1-\left[\omega-\frac{\omega_m}{\Delta\omega}\right]^2\right]^2 \tag{12}$$

can also be used. This filter reduces the amplitude of the first sidelobe in the time domain to parts in 10^2 but still has the advantage of having well-defined cutoff frequencies.

This leaves approximately the following signal:

$$V=E_p(t)E_{\mathrm{cw}}^{*}e^{-i\omega_m t}. \tag{13}$$

Since E_{cw}^{*} is constant in time, it represents only an overall phase, which is not of interest here, and an amplitude scale, which may be normalized if necessary by measuring the pulsed and cw laser intensities. The complex exponential factor serves only to shift the spectrum of the signal by $+\omega_m$. This offset is eliminated by shifting the spectrum down in frequency to place its measured center of gravity at the origin. We now have determined the complex electric field envelope which completely characterizes the laser pulse. The squared magnitude of the complex envelope gives the pulsed laser intensity profile, and the arc tangent of the ratio of the imaginary and real components gives the phase as a function of time; the derivative of the phase then gives the instantaneous frequency versus time $F(t)$.

C. Testing the algorithm

The ultimate test of this entire measurement technique would be to characterize a pulsed laser as described and predict a line shape for a simple experiment involving nonlinear spectroscopy. In lieu of this ideal, we have taken several steps to test the measurement and reconstruction algorithm. As described in Sec. V, we have been able to reproduce the effects of filtering our laser pulses in a Fabry-Pérot filter. In addition, we have taken advantage of the similarity of our laser system to that used by Hildum *et al.* [3] to calculate a two-photon line shape and shift in good agreement with that found in their work.

To better understand the sources and magnitude of error in the frequency reconstruction process, the procedure was tested numerically. At the simplest level, it was determined that the procedure recovers the frequency versus time of a Gaussian pulse with various frequency chirps. The linear chirp of a simulated chirped Gaussian pulse is reconstructed exactly within the numerical limits of the computer. For this case, however, the low-frequency intensity terms are very well separated from the interference term at ω_m, and the conditions for the exact reconstruction of the instantaneous frequency of the pulse are met. Experimentally, however, it is difficult to precisely meet these requirements.

The experimentally measured intensity profile $I_{\mathrm{exp}}(t)$ of a pulse from our pulsed amplifier is shown in Fig. 1(b); its corresponding Fourier transform is shown in Fig. 5. It can be seen that there are high-frequency components in this intensity profile throughout the bandwidth of the detection system. For the excimer-pumped dye-amplifier system used here, these high-frequency components may

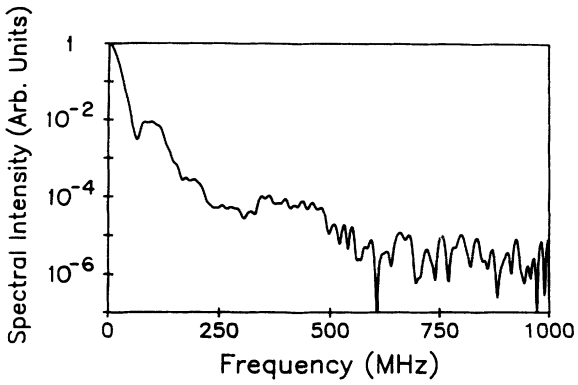

FIG. 5. Fast-Fourier transform of the experimentally measured intensity profile of an excimer-pumped dye-amplifier pulse. The intensity profile is shown in Fig. 1(b).

be dominantly associated with the sharp rising edge of the pulse. Thus the primary source of error in this reconstruction process is the overlap of the high-frequency components of the intensity profile with the beat note frequency components. Thus our heterodyne technique will work much better with a smooth laser intensity profile (e.g., a Gaussian pulse), since there are fewer high-frequency components to overlap with the interference term.

We determine the degree to which these laser intensity fluctuations affect our instantaneous frequency measurement in the following way. We numerically simulated the heterodyne beat note that we would measure with an exactly Fourier-transform-limited laser pulse with the same intensity profile as that of our excimer-pumped laser:

$$V_{\text{synth}} = I_{\text{expt}}(t) + [I_{\text{expt}}(t)]^{1/2}\cos\omega_m t$$
$$= I_{\text{expt}}(t) + \tfrac{1}{2}(I_{\text{expt}})^{1/2}(t)e^{-i\omega_m t}$$
$$+ \tfrac{1}{2}(I_{\text{expt}})^{1/2}(t)e^{i\omega_m t}. \quad (14)$$

The procedure described above was then used to reconstruct the frequency versus time of this pulse. Ideally, the reconstruction of this pulse should yield a constant instantaneous frequency. The results are shown in Fig. 6(b) for a beat frequency $\omega_m = 380$ MHz and bandpass half-width $\omega_m/2$. Except for the large deviations at the rising and trailing edges, there is a deviation from a constant intantaneous frequency that fluctuates to ± 2 MHz throughout the phase.

To demonstrate that this deviation is caused by frequency components of the intensity term at the beat frequency, the first term in (14) is removed. The frequency reconstruction then appears as in Fig. 6(c). The noise at the rising and trailing edges persists. However, between the 10% intensity points the deviation is less than ± 0.5 MHz from the ideal constant frequency. We believe that the deviation at the rising and trailing edges of the pulse is due to weak sidelobes introduced in the time domain by our frequency domain filtering process.

In conclusion, we have determined that the total level of noise, or error, in our heterodyne frequency measure-

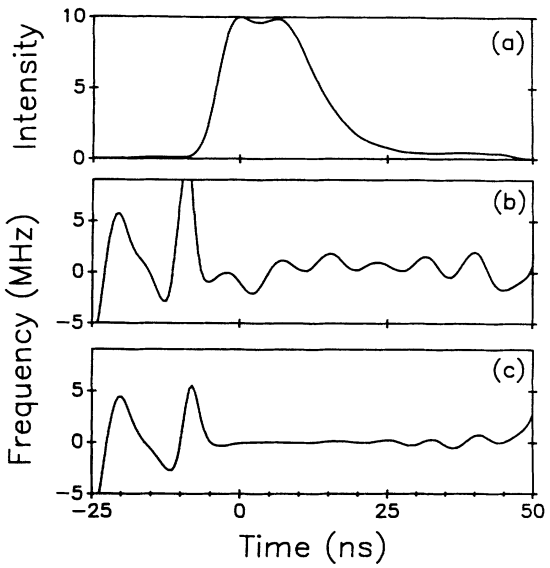

FIG. 6. (a) Reconstructed instantaneous intensity. For comparison, Fig. 1(b) shows an experimentally measured intensity profile. (b) Frequency vs time of a synthesized heterodyne signal: $V_{\text{synth}} = I_{\text{expt}}(t) + (I_{\text{expt}})^{1/2}(t)\cos\omega_m t$. This demonstrates the error in the frequency reconstruction (± 2 MHz between the 10% intensity points) introduced by the overlap of intensity profile frequency components (Fig. 4) with the interference term. If there were no overlap, the result would be a constant zero frequency. (c) shows the frequency reconstruction with no intensity term added into the synthesized beat note. The noise at the rising and trailing edges of the pulse is due to the filtering process used in the algorithm.

ments is roughly ± 2 MHz, or roughly 1.3 MHz rms, between the 10% intensity points. Figure 7 shows the typical $F(t)$ of several laser pulses for several beat frequencies. The zero frequency of these curves is referenced to

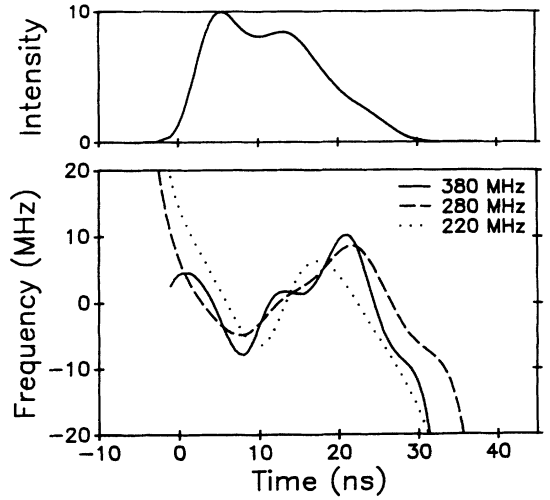

FIG. 7. Reconstructed instantaneous frequency vs time of an excimer-pumped dye-amplifier pulse measured with three different beat frequencies: 220, 280, and 380 MHz. Zero frequency is referenced to the center of gravity of the spectrum of each pulse. The intensity curve is the reconstructed intensity profile of the 380-MHz pulse.

the center of gravity of the spectrum of the pulse. The 20-MHz frequency excursions found in these measurements are independent of beat frequency and are thus not associated with a particular feature in the noise spectrum. These features are presumed to be real.

IV. EXPERIMENTAL RESULTS

There are several interesting features of the pulsed amplifier output that we will discuss. We have not attempted to systematically characterize the spectral behavior of our pulsed dye-amplifier laser under a number of different conditions. Rather we present only a few preliminary measurements.

It has long been known that the spectrum of the pulsed amplifier output is not centered at the seed beam frequency. For our laser system, this is typically offset by as much as 25–45 MHz to the blue, depending on a number of factors including amplifier alignment and the number of amplifier stages. This shift is irrelevant to the previous discussion on the two-photon transition since the spectrum of the pulsed light may be easily measured using an optical spectrum analyzer. For purposes of making this measurement, the heterodyning technique offers one advantage over using a spectrum analyzer. The spectrum of individual pulses may be determined, as opposed to the average spectrum of an ensemble of pulses. The pulse-to-pulse jitter of the center frequency of the pulse spectrum relative to the seed beam is found to be nearly 1 MHz rms.

This jitter may be important if there is any correlation between frequency jitter and amplitude jitter. Such a correlation may be significant in a precision pulsed measurement since even if the individual pulses are Fourier-transform limited, the center of the two-photon spectrum would not correspond to the center of the average pulse spectrum. This effect is not significant at the 1-MHz level since the pulse-to-pulse frequency jitter is ~ 1 MHz rms and the intensity jitter is $\sim 10\%$. Even with perfect correlation this leads to a shift on the order of ~ 100 kHz.

We have measured the complex electric field envelope $E(t)$ of our laser pulses under several experimental situations. The frequency behavior of these pulses was characterized by determining the relative shift between the spectral intensity profile of $E(t)$ and that of $E^2(t)$, as discussed in Sec. II. To determine the pulse-to-pulse reproducibility of this "E^2 shift," the shift was determined for a series of ten nearly consecutive pulses. The jitter in the E^2 shift was roughly 3 MHz rms. The average intensity and frequency behavior of these ten pulses was determined by averaging the reconstructed intensity and frequency versus time of each pulse. An "average pulse" was created using the resulting intensity and frequency variations. The E^2 shift of the "average pulse" was found to be within 1 MHz of the mean E^2 shift of the individual pulses. We estimate that at the 1-MHz level it is necessary only to determine the average frequency behavior of the pulsed laser for any given set of experimental conditions: pump power, amplifier alignment, number of stages, laser wavelength. After "retweaking" the amplifier alignment, the frequency behavior changes by a significant amount.

The explanation of the shift of the laser spectrum from the seed frequency, and of frequency chirps within the pulse, has been based on the argument that fluctuations in the gain medium of the amplifier lead to index-of-refraction fluctuations. The time derivative of the index of refraction leads to a Doppler-like frequency shift. One consequence of this argument is that the magnitude of the shift and chirps should have some dependence on the position of the laser frequency under the gain curve of the gain medium, but we have not made an estimate of the expected size of the effect. We have looked for the dependence of both the center frequency and the E^2 shift of the pulses on the laser wavelength, but no statistically significant correlation was found.

V. EFFECT OF FABRY-PÉROT FILTER ON LINE SHAPE AND SHIFT

It has been implicitly assumed in the literature of the field of precision laser spectroscopy that the phase noise inherent in pulse amplification can be removed from a laser pulse using a narrow optical bandpass filter such as a Fabry-Pérot filter. The optical pulse builds up the filter-cavity resonance, which subsequently rings down with the characteristic decay time of the cavity, producing a light pulse that may be spectrally much narrower than the unfiltered pulse. The assumption has been that the light emitted by the filter cavity during this process is sufficiently Fourier-transform limited that a precision measurement will not be disturbed. This is an erroneous assumption: the process of filtering a laser pulse can itself introduce a large error into a precision frequency measurement.

The transfer function of a Fabry-Pérot filter is given as [16]

$$\Gamma(\omega)=\frac{1-R}{1-Re^{i\tau_{\mathrm{RT}}\omega}} \tag{15}$$

where R is the intensity reflectivity of each cavity mirror, $\tau_{\mathrm{RT}}=2L/c$ is the cavity round-trip time, and ω is angular frequency. Given an arbitrary incident field envelope, the transmitted electric field envelope may be calculated numerically using the transfer function (15). The instantaneous frequency characteristics of the transmitted pulse can then be determined from the phase of the transmitted field. This is done for an incident field given by a three times Fourier-transform-limited Gaussian pulse with a linear chirp. The frequency and amplitude behavior of the transmitted pulse is shown in Fig. 8.

The transmitted field is clearly not Fourier-transform limited, and in fact contains a large frequency chirp on the leading edge of the pulse. The frequency subsequently oscillates as it approaches the resonant frequency of the filter cavity. In light of the previous discussion of the effects of frequency chirps on the two-photon line shape, we see that if this pulse were used to excite this transition, the low frequency at the peak intensity of the pulse would be relatively enhanced, shifting the line to the blue in the resulting spectrum. This frequency behavior is

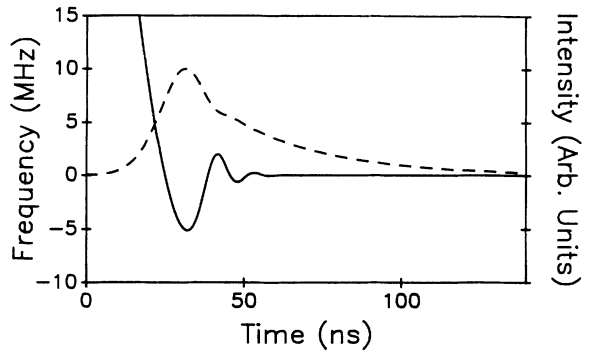

FIG. 8. Numerical calculation of the instantaneous intensity (dashed curve) and frequency (solid curve) versus time of a Fabry-Pérot filtered Gaussian pulse. The Gaussian pulse is three times Fourier-transform limited [80 MHz full width at half maximum (FWHM)] with a linear frequency chirp. The filter has a bandwidth of 5 MHz and a finesse of 40. Note the megahertz excursions of the frequency that extend well past the peak of the filtered pulse.

clearly not desirable for precision spectroscopy. The leading edge of the filtered pulse can be removed with a Pockel cell so that the portion of the filtered light with the most troublesome frequency chirps is eliminated. However, Fig. 8 shows that it would be necessary to remove most of the peak of the filtered pulse to significantly reduce this effect.

We have experimentally measured the instantaneous frequency of a pulsed laser filtered by a Fabry-Pérot resonator. The pulsed laser is approximately mode matched to the TEM_{00} mode of a confocal cavity of length $L=75$ cm ($\tau_r=5$ ns) and a finesse of approximately 40 (reflectivity of 92.5%). This gives a free spectral range of 200 MHz and a bandwidth of 5 MHz. The actual bandwidth of the filter with our pulsed laser was nearly 8 MHz, indicating excitation of high-order transverse modes due to inexact mode matching. The high-order transverse modes are not precisely degenerate due to spherical abberation and slight nonconfocality of the resonator. The resonator was locked to an off-axis cw beam using a frequency modulation technique. The pulsed output of the resonator is attenuated and directed with the reference laser onto the detector. The resonator can be removed to measure the unfiltered laser pulse as well.

Figure 9 shows the resulting signal and its Fourier transform for a filtered pulse. The intensity (filled circles) and instantaneous frequency (open circles) of the filtered pulse were extracted by the described algorithm and are shown in Fig. 10. To test the frequency measurement technique we digitally filter the measured electric field of an unfiltered laser pulse with the filter represented in (15), and compare this with the measured electric field of the Fabry-Pérot filtered laser pulse. The digitally filtered pulse is also shown in Fig. 10 (solid lines), and can be seen to be nearly identical to the optically filtered pulse.

An interesting feature in these results must be pointed out. When these data were taken, the spectral peak of the unfiltered laser pulse (as read directly from the

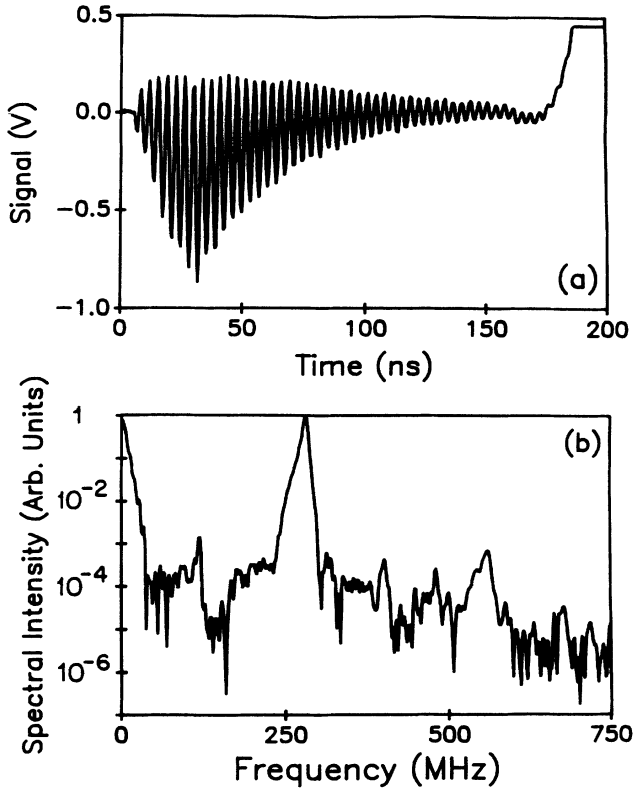

FIG. 9. (a) Typical heterodyne signal of Fabry-Pérot filtered dye-amplifier pulse. Digitized points (not shown) are at 0.5-ns intervals. The feature at the end of the signal is due to the cw reference beam being turned off. (b) The fast-Fourier transform of the heterodyne signal shows the intensity term at dc and the interference term at 280 MHz. The small feature at 560 MHz is due to slight saturation of the detector.

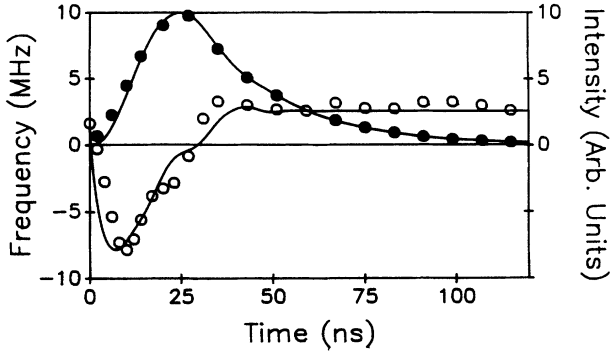

FIG. 10. Reconstructed instantaneous intensity and frequency vs time of Fabry-Pérot filtered pulses. The filled and open circles show the intensity and frequency, respectively, of a laser pulse that is experimentally Fabry-Pérot filtered, and then heterodyned and digitized. The solid lines show the intensity and frequency of an amplified laser pulse that is heterodyned and digitized, and then filtered numerically with the Fabry-Pérot transfer function. The solid lines are *not* a fit to the circled points. The real and numerical filters are offset +13 MHz from the peak frequency of the unfiltered light.

Fourier transform of the interference signal) was roughly 13 MHz to the red of the center of the Fabry-Pérot filter. This is because the acousto-optic modulator that gates the seed beam was set at −42 MHz, overcompensating for the roughly +30-MHz center frequency shift the pulsed amplifier imparts during amplification. The result of this 13-MHz frequency offset is the large frequency chirp that appears near the peak intensity of the filtered pulse.

We have numerically investigated this effect for the case of a Fourier-transform-limited Gaussian pulse. The frequency behavior shown in Fig. 11(b) is determined by multiplying a Gaussian frequency spectrum by the Fabry-Pérot transfer function (15) placed off center by $\nu_0 = 12$ MHz. The explanation for this chirp is straightforward. At times less than the round-trip time of the cavity, there is no interference, so the transmitted light pulse must begin at the center frequency of the driving field. At long times, after the driving pulse has died away, the resonator is ringing down at its natural resonance frequency. Since these are different frequencies when the filter is placed off center, there must be a chirp in the transmitted pulse. The zero frequency here is referenced to the center of gravity of the spectrum of the transmitted pulse.

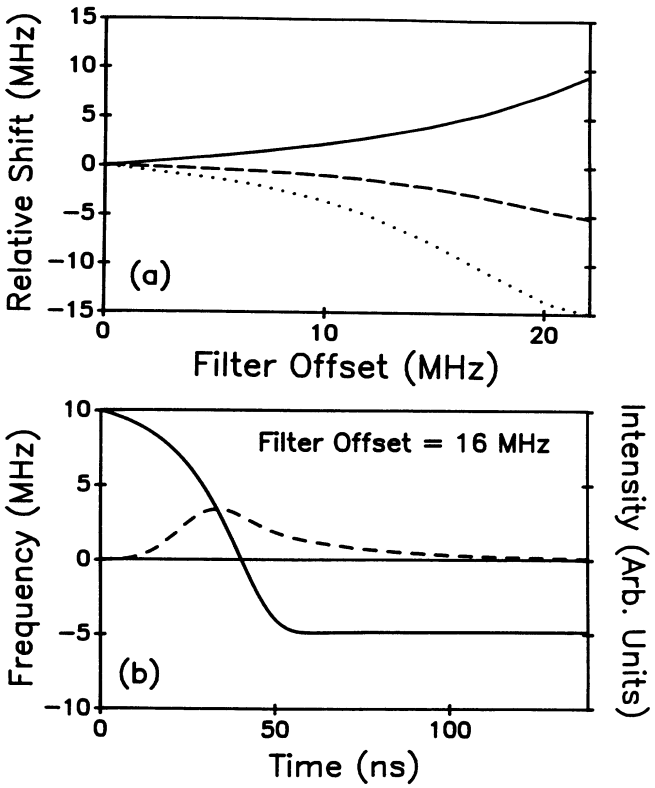

FIG. 11. Effect of filtering a Fourier-transform-limited Gaussian pulse with an offset between the spectral peak of the pulse and the peak of the Fabry-Pérot filter. The spectral width of the pulse and filter are 27 and 5 MHz FWHM, respectively. (a) The solid curve is the center of gravity (CG) of the filtered light relative to the filter center. Also shown is the shift produced in the two-photon line center when the filtered light is used directly to drive the transition (dashed curve), and when the filtered light is doubled using second-harmonic generation before driving the transition (dotted curve). (b) The instantaneous intensity and frequency of the filtered pulse is shown for a filter offset of 16 MHz. Note that at the peak of the pulse, the frequency is at +3.5 MHz. A two-photon transition will respond to this pulse as if it were at a higher average frequency than its spectral peak, requiring a negative detuning to get a peak atomic response.

The effect of this chirp is significant in a two-photon transition. It is clear that the instantaneous frequency at the peak intensity (temporally) of the pulse is well above the center frequency of the resonator (given by the long exponential tail of the transmitted pulse). As a result, the two-photon transition responds to the pulse as though it were at a higher frequency than indicated by its power spectrum. The resulting shift in the CG of the two-photon line shape from the CG of the incident field is shown in Fig. 11(a) (dashed curve) as a function of the relative offset ν_0 of the Fabry-Pérot filter. The shift down is due solely to the presence of E^2 in the interaction potential. All of the simplifying assumptions discussed in Sec. II A are in place.

A. Effect of harmonic generation

The process of frequency doubling the pulsed laser by second-harmonic generation (SHG) may also leave the spectroscopist vulnerable to the deleterious effect of frequency chirps. This is relevant since a prime motivation for employing pulsed lasers for spectroscopy is the relative ease of producing coherent ultraviolet radiation by SHG. In the limit that the bandwidth of the pulse is sufficiently narrow that phase-matching and dispersion effects can be neglected, the electric field of light produced by SHG is proportional to the square of the driving electric field. Again, in view of the previous discussion on the effect of the E^2 in the interaction potential of a two-photon transition, it is clear that SHG will produce similar shifts in the center of gravity of the doubled light that must be taken into consideration, even when the transition under study is a one-photon transition.

When the observed transition is second order in the atom-field interaction, the line shape is proportional to the power spectrum of $E^4(t)$ and the effect of frequency chirps is greatly enhanced. Figure 11(a) (dotted curve) also shows the shift in the two-photon line for the case of the off-center filtering of the Gaussian pulse (discussed above), where the exciting laser pulse has first been frequency doubled. These shifts are still referenced to the center of gravity of the filtered, undoubled pulse, and the frequency scale is twice that of the doubled light. The shifts shown in Fig. 11(a) indicate the problems inherent in an experiment where the metrology is done on the fundamental frequency, while the spectroscopy involves a sum or a higher harmonic of this light. We will further discuss this point later.

B. Correction to a pulsed measurement of the hydrogen 1*s*-2*s* interval

This discussion is relevant to a recent pulsed measurement of the 1*s*-2*s* two-photon transition in hydrogen which is in disagreement with theory and other (cw) measurements by roughly −18 MHz [3]. In that experiment,

an excimer-pumped (10-ns pulse width) dye amplifier was seeded with a stabilized ring laser operating near 486 nm. The seed beam was used to frequency lock a Fabry-Pérot resonator ($\tau_{RT}=1.5$ ns, finesse of 40) that served to reduce the 180-MHz width of the amplified pulse to ~15 MHz. The filtered pulse was then frequency doubled to generate the 243-nm light used to excite the hydrogen two-photon transition. In that experiment, no attempt was made to place the filter at the center of gravity of the amplified laser pulse.

We have modeled the 10-ns dye-laser pulses by multiplying the time scale of the measured electric field of our 20-ns laser pulses by a factor 2, increasing the frequency width to ~70 MHz. The relative shift between the filter-cavity locking beam and the transmitted pulse was measured in the hydrogen experiment to be approximately 4 MHz to the blue, giving an indication of the relative shift between the filter cavity and the unfiltered laser pulse. When we displace our model pulse by ~30 MHz to the blue of our digital filter, the CG of the upper half of the transmitted pulse is 3.5 MHz to the blue of the filter-cavity center frequency, in good agreement with the 4-MHz blue shift in the CG of the upper half of the laser spectrum measured in the hydrogen experiment.

The electric field of the digitally filtered model pulse is then squared to find the electric field of the doubled pulse and then squared again to obtain the two-photon line shape. This model predicts a shift of the line by −5 MHz in the blue, and thus a shift of $-20(\pm 10)$ MHz in the measured $1s$-$2s$ splitting, nicely accounting for the observed $-18(\pm 5)$-MHz discrepancy. The error bars on our correction reflect our lack of knowledge about the actual pulses used in this experiment. Our predicted line shape is shown in Fig. 12 superimposed on an experimental line obtained in the hydrogen experiment. Note that the predicted line shape has the same tail toward red as the experimental line. The experimental line is slightly broader than the predicted line, indicating the presence of power broadening not included in our model.

In the positronium experiment [4] the filter was centered with respect to the pulsed light, and the corrections

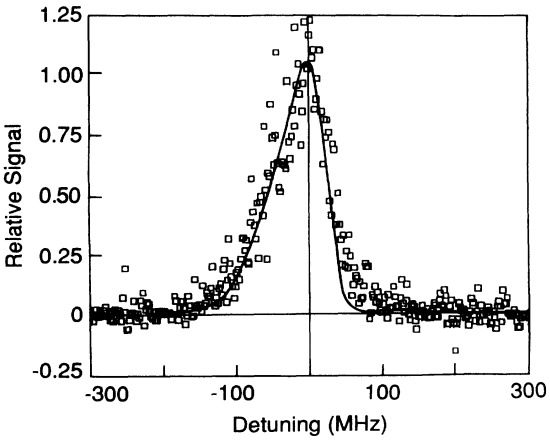

FIG. 12. Predicted line shape for the recent pulsed hydrogen experiment. (Hildum *et al.*) The raw laser pulse is 30 MHz to the blue of the center of the Fabry Pérot filter. Note that the asymmetric tail on the red side of the transition is predicted.

are on the order of 1–2 MHz. In the muonium experiment [5], the light was not filtered with a Fabry-Pérot interferometer.

VI. DISCUSSION

As compared to our current error estimate of 1.3 MHz rms, we believe it is not reasonable to expect an accuracy of better than 0.1 MHz rms in the instantaneous frequency measurement with the current experimental setup. There are several routes one may take to achieve this improved accuracy. The leakage of the pulsed laser intensity term into the interference term is a dominant source of error in the present measurement. Note also that the magnitude of the frequency components of the intensity term decrease rapidly between 10 and 500 MHz, and appears to level off at −40 dB at higher frequencies. Although at present the spectrum of the pulsed dye-laser intensity is unknown at frequencies greater than 1 GHz, it is likely that a beat note at 1 GHz would result in improved accuracy.

It is probable that the excimer laser contains intensity noise at even higher frequencies due to mode beating under its relatively large bandwidth. Although the dynamics of the excited-state population of the dye amplifier will tend to wash out these high frequencies, the advantages of going to a beat note even higher than 1 GHz are as yet unclear.

One straightforward way around the problem is to use a pump laser with a smooth temporal pulse. For example, a Nd:YAG (where YAG denotes yttrium aluminum garnet) laser seeded with a cw diode pumped Nd:YAG oscillator has a roughly Gaussian temporal pulse with no high-frequency components that would overlap with the true heterodyne beat note.

The limited detection bandwidth of the interference term is also a source of error. The bandwidth we were able to achieve (380 MHz) could also be improved by using a higher beat note, bandpass filtering the interference term electronically, and mixing the interference term down to the center of the digitizer bandpass (500 MHz) [17]. We could then take advantage of the full 1-GHz bandwidth of the digitizer.

Another entirely different approach to the problem of extracting phase information from a heterodyne signal is to make a simultaneous measurement of the pulsed laser intensity, in addition to the heterodyne signal already measured. Recalling Eq. (11), we note that the measured intensity can be used to subtract from the heterodyne signal the offending term $I_p'(t)$. This contains both the signal intensity and ASE intensity whose high-frequency components leak into the interference term to disturb the phase measurement. The remainder of the algorithm would be unchanged: bandpass filter the positive frequency part of the interference term to recover the complex electric field envelope.

The simultaneous intensity and heterodyne measurements can be made with two separate detectors with the disadvantage of having to simultaneously digitize two channels of signal, using up scarce and expensive sampling rate. The measurement can also be done with a single detector by delaying a piece of the pulsed light by

~50 ns and directing it onto the heterodyning detector with its polarization rotated by 90° to prevent interference with the cw reference beam.

The technique has the advantage that the intensity terms may be removed regardless of the high-frequency components present, making itself useful for cases of very noisy intensity profiles. However, if the complex electric field envelope is to be recovered by bandpass filtering the positive frequency part of the interference term, the positive and negative parts must be spectrally well separated. Since these contain the same high-frequency components associated with the pulse intensity, this again requires a high-frequency beat note, although it need only be half as high as when the intensity term is not subtracted out.

The constraint may be removed entirely by attempting to normalize the third term in (10) by the measured electric field magnitude $(I_p')^{1/2}(t)$. Of course, this is only possible if the measured quantity $I_p'(t)$ is identical to $I_p(t)$ and contains no contribution from $I_{\rm ASE}(t)$. Toward this end, the pulsed light can be passed through a monochromator before it is heterodyned to remove the ASE intensity term from both the heterodyne signal and the intensity measurement. The third term in (10) can then be normalized by the measured electric field magnitude, leaving $\cos\phi(t)$. The acr cosine of this quantity yields the relative phase of the pulsed light, the derivative of which is the instantaneous frequency.

There are several disadvantages with this technique that must be discussed. First, it is very sensitive to the response of the two detectors both at low frequencies, where the intensity terms lie, and at higher frequencies around the interference term. This is accentuated by the fact that at the rising and trailing edges of the pulse, normalizing the third term in (10) requires dividing one small signal by another small signal, both of which have limited accuracy. Thus the complex transfer function (or impulse response) of the detector(s) must be precisely measured either to verify that it is sufficiently constant or to enable us to deconvolve the impulse response from the signal.

The technique also requires that the pulsed laser beam be well spatially filtered since any spatial inhomogeneity in the beam will mean that the detector measuring the pulse intensity and the detector measuring the heterodyne signal may not see the same part of the pulsed beam. The resulting instantaneous frequency measurement would thus be erroneous. Although this requirement is still valid for the present experimental situation, the measured electric field is accurate at the point measured, but may not represent the electric field at other transverse locations on the pulsed beam.

VII. CONCLUDING REMARKS

We have theoretically investigated the effect of frequency chirps on a two-photon transition and found that the line shape of this transition is strongly dependent on the spectral character of the excitation pulse. In particular, the line shape and line center of the two-photon spectrum are not equivalent to the spectral shape of the exciting laser pulse. Thus detailed knowledge of the complex electric field of the laser pulse is necessary to make precise wavelength measurements using pulsed spectroscopy for nonlinear transitions. We have determined the extent of this effect for several simple cases, including the case of our own seeded pulsed dye-amplifier system. With this model, we have proposed an explanation for the discrepancy with theory of a recent pulsed measurement in hydrogen.

We have demonstrated an experimental and signal processing technique to determine the instantaneous electric field of a seeded pulsed dye amplifier (and have determined some interesting features in this system). The technique should be directly applicable to many other pulsed laser systems used in spectroscopic measurements, although there are some constraints. Primarily, the Fourier components of the laser pulse must lie in a sufficiently narrow frequency band that when the pulse is heterodyned with a reference laser, all the frequency components of interest can be detected and digitized in a single shot. For practical purposes, this limits the laser bandwidth to several hundred megahertz, such as in our laser system where 90% of the laser is within 100 MHz. However, it is conceivable, with state-of-the-art digitizer technology, to extend the measurable laser bandwidth limit to 1 GHz or higher.

The present work has implications on the application of cw lasers to precision spectroscopy and to cw atomic clocks. Precision measurements with cw lasers often involve both nonlinear (e.g., two-photon) transitions [7,8] and/or the generation of the clock frequency by sum frequency mixing or harmonic generation [18]. In addition, the previous frequency up conversion of the Cs standard to the methane line at 3.39 μm required a cascade of nonlinear devices [19], and a recently proposed method of visible frequency division [20] will require a cascade of nonlinear devices to generate frequencies of the form $f_3=(f_1+f_2)/2$. The main result of this paper can be simply put: if there is a correlation between the frequency chirp and the intensity fluctuations of the laser or microwave source, there will be a shift in the centroid of the nonlinear response with respect to the centroid of the frequency spectrum. For a laser frequency based on a nonlinear interaction, this correlation can occur in a natural way. For example, if the doubling crystal phase matching not centered with respect to the input frequency or if there is an offset between the buildup cavity center frequency and the frequency of the injected light, frequency excursions of the second harmonic will be automatically correlated to amplitude fluctuations. The use of the second-harmonic frequency in ultraprecise spectroscopy will cause an error in the measurement unless accounted for. This error may be small but still significant for applications such as cw atomic clocks where the measurement precision is expected to reach parts in 10^{18}.

ACKNOWLEDGMENTS

This work was supported in part by the National Science Foundation and in part by a National Institute of Standards and Technology Precision Measurements Grant. It is a pleasure to acknowledge enlightening discussions with R. G. DeVoe, J. L. Hall, T. W. Hänsch, E. A. Hildum, and P. J. Ungar. We are also grateful to E. A. Hildum for supplying samples of his original data.

*Present address: Max-Planck-Institut für Quantenoptik, D-8046 Garching, Federal Republic of Germany.

[1] C. E. Wieman and T. W. Hänsch, Phys. Rev. A **22**, 192 (1980).

[2] T. W. Hänsch, S. A. Lee, R. Wallenstein, and C. Wieman, Phys. Rev. Lett. **34**, 307 (1975).

[3] E. A. Hildum, U. Boesl, D. H. McIntyre, R. G. Beausoleil, and T. W. Hänsch, Phys. Rev. Lett. **56**, 576 (1986).

[4] Steven Chu, Allen P. Mills, Jr., and John L. Hall, Phys. Rev. Lett. **52**, 1689 (1984).

[5] Steven Chu, A. P. Mills, Jr., A. G. Yodh, K. Nagamine, Y. Miyake, and T. Kuga, Phys. Rev. Lett. **60**, 101 (1988).

[6] J. R. M. Barr, J. M. Girkin, J. M. Tolchard, and A. I. Ferguson, Phys. Rev. Lett. **56**, 580 (1986).

[7] R. G. Beausoleil, D. H. McIntyre, C. J. Foot, E. A. Hildum, B. Couillard, and T. W. Hänsch, Phys. Rev. A **35**, 4878 (1987).

[8] M. G. Boshier, P. E. G. Baird, C. J. Foot, E. A. Hinds, M. D. Plimmer, D. N. Stacey, J. B. Swan, D. A. Tate, D. M. Warrington, and G. K. Woodgate, Nature (London) **330**, 463 (1987).

[9] Max Born and Emil Wolf, *Principles of Optics,* 6th ed. (Pergamon, New York, 1987), Chap. 10. In general, the power spectrum of optical fields is given as the Fourier transform of the time-averaged correlation function. This form is most appropriate for a continuous light source whose field can be represented by a stationary, ergodic random variable. However, for a pulsed laser field, which has finite time extent, the power spectrum is most intuitively expressed in the form shown. The complex representation of real fields is discussed in this reference as well.

[10] R. G. Beausoleil and T. W. Hänsch, Phys. Rev. A **33**, 1661 (1986).

[11] B. R. Mollow, Phys. Rev. **175**, 1555 (1968). Mollow gives a general result for the two-photon transition probability for arbitrary excitation fields.

[12] G. C. Bjorklund, Opt. Lett. **5**, 15 (1980).

[13] J. L. Hall, L. Hollberg, T. Baer, and H. G. Robinson, Appl. Phys. Lett. **39**, 680 (1981).

[14] D. Herriott, H. Kogelnik, and R. Kompfner, Appl. Opt. **3**, 523 (1964).

[15] For a collimated beam entering the final amplifier stage, the spatial Fourier-transform plane of the amplified light appears at a distance much larger than the Rayleigh range of the beam. This is inconveniently large for our 3-mm output beam. If, however, the beam entering the final amplifier stage has a radius of curvature 6 m away, the spatial Fourier transform of the amplifier stage appears at this distance.

[16] Max Born and Emil Wolf, *Principles of Optics,* 6th ed. (Pergamon, New York, 1987), p. 325.

[17] T. W. Hänsch (private communication).

[18] Wayne M. Itano, J. C. Bergquist, and D. J. Wineland, Science **237**, 612 (1987).

[19] D. A. Jennings, C. R. Pollock, F. R. Peterson, R. E. Drullinger, K. M. Evenson, J. S. Wells, J. L. Hall, and H. P. Layer, Opt. Lett. **8**, 136 (1983).

[20] H. R. Telle, D. Meschede, and T. W. Hänsch, Opt. Lett. **15**, 532 (1990).